



Two-time level finite-difference method for solving the downstream diffusion for flow between Parallel plates

Original
Article

Hany Saad¹, Hamada G. Asker²

¹Departments of Mechanical Power Engineering and ²Math and Physics, Faculty of Engineering, Ain Shams University, Cairo, Egypt

Keywords:

Convection heat transfer, downstream diffusion, parallel plates, Nusselt number.

Corresponding Author:

Hany Saad, Department of Mechanical Power Engineering, Faculty of Engineering, Ain Shams University, Tel.: 01000385638, Email: hany.elsayed@eng.asu.edu.eg

Abstract

The heat transport equation for laminar flow between isothermal parallel-plate channels in the entrance region is solved numerically. The heat transport equation is solved using the rightward representation of Barakat-Clark ADE method. The proposed numerical method uses the two-time levels derivative to solve the unsteady term in the transport equation. The unsteady term presented using two-time level derivative at n and $n+1$ combined with backward derivative i and $i-1$. The heat equation contains the unsteady term and the axial heat term. The heat transfers within flow between two parallel plates. The results for the local Nusselt number, the mean temperature, and thermal entry length is shown. The analysis provides the temperature distribution considering the axial heat conduction and the downstream diffusion. The results show the effect of the upstream on the inlet temperature and ensure the reliability of the proposed numerical method to solve the transport equation including the unsteady term and the two-dimensional partial derivative.

1. INTRODUCTION

Gratz-Nusselt problem is a well-known problem as a T-problem where the flow is fully developed and uniform temperature at the inlet. This case exists in the heat exchangers of finite length with good mixing in the headers at the inlet and outlet.

For the fluid heating ($T_w > T_{fluid}$) where T_w is "wall temperature", the effect of fluid axial conduction should be included in the study to avoid the error of calculations. While heating, part of the heat is transferred from the walls raising the local enthalpy, and the rest is consumed in heating the incoming fluid at the header's inlet ($-\infty < x < 0$) by conduction. Preheating the upstream fluid affect the temperature distribution at the inlet condition at $x = 0$, the inlet temperature will not be uniform while including the fluid axial conduction. So neglecting the fluid axial conduction may cause calculation error especially at low Peclet numbers.

The upstream and downstream regions of the flow between parallel plates are solved using a series-solution^[1]. The study included fluid axial conduction. The solution presents a good approach long away from the entrance due to the difficulties in evaluating the eigen values. While near the entrance the solution fails (smallest values of axial distance). Allem's scheme is then applied^[2] considered the steady-state energy equation downstream considering the fluid axial conduction. The presented

results deviate from Great solution^[3] for $X^* = (x/De)/Pe < 0.0025$ with deviation up to 25 %. Good agreement with Graetz solution for $X^* = (x/De)/Pe > 0.0025$. The results of both the local bulk temperature and the local Nusselt number presented graphically for Pe "Peclet" numbers up to 10^6 .

The problem is solved again^[4] using a closed-form using a Second-, Third-, and Fourth-order polynomial for the temperature and Nusselt number. The third-order polynomial presented the lowest deviation from the exact solution. However, the calculations at small still very difficult when the fluid axial diffusion is considered. In 1973, they presented^[5] the same problem in considering the effects of the upstream and the downstream conditions on the heat transfer with the fluid axial conduction.

The solution extended to regions ($-\infty < x < \infty$) using the central finite-difference^[6] to solve the steady-state energy equation. He stated that the effect of the axial conduction cannot be formulated by simply adding the axial conduction term to the energy equation while using a semi-infinite duct with uniform inlet temperature. Also, the axial conduction effect is more pronounced in the case of constant wall temperature, and the axial effect may be neglected for $Pe > 50$. The study mentioned that the fluid axial conduction can cause a considerable increase in the thermal developing length. An exact solution presented^[7] to show the temperature distribution, the velocity profiles, and the local Nusselt number for slug flow and for both

upstream and downstream regions. The results found that the heat transfer characteristics are sensitive for Biot number and Peclet number in the thermal entrance region.

The ADI method^[8] demonstrated the convergence by definite error and the results presented the local Nusselt number for $X^* < 0.0025$ [ref, table 7, 8]. Also, it presented the thermal entry length for Peclet number up to 1000. Then considered^[9] the forced convection in a parallel plate channel filled with a saturated porous medium to present modified Graetz methodology considering the fluid axial conduction, and viscous dissipation. The solution presented dimensionless expressions for the local Nusselt number as a function of the dimensional longitudinal coordinate and other parameters (Darcy number, Peclet number, Brinkman number). A numerical study for asymmetric heating^[10] stated that the Nusselt number is independent of the asymmetry if and only if the velocity profile is symmetric with respect to the midline of the channel. The axial heat conduction in parallel flow microchannel heat exchanger^[11] mentioned that increasing the Reynolds number Re and thermal conductivity K leads to an increase in the axial heat conduction while increasing hydraulic diameter D_h and channel volume leads to a decrease in the axial heat conduction.

The study^[12] considered constant wall temperature considering axial conduction. The results showed that considering the axial conduction increases the local Nusselt number Nu_x . Considering the fluid axial conduction increases the heat transfers to the wall and this effect decreases obviously as Peclet number increases. The axial effect^[13] within micro-channels the local Nusselt number at infinity is Nu_{To} for constant temperature for flow between two parallel plates. The study presented a derived correlation

for the Nusselt number. A mathematical approach^[14] is used to evaluate the effect of flow maldistribution in a parallel plate-fin heat exchanger. Another numerical study^[15] on the motion of a magnetorheological fluid under the application of a magnetic external field in modifying the velocity profile and the pressure drop along the channel show good results.

The instability of pure Newtonian fluid flow between two parallel plates^[16], where the bottom one coated with various porous media with permeability and porosity is investigated. A numerical solution^[17] analyzed numerically the fully developed laminar flow of the Cross fluid between parallel plates under uniform heat flux. Fredrik and Trygve^[18] presented an experimental and numerical study for the hydrodynamic loads on two-dimensional perforated plates.

In this paper, the numerical solution extends the rightward representation of^[19-20] method to present a result of the developed flow in the entrance region of parallel plates, and laminar forced convection as shown in figure 1 and 2. The flow is fully developed, and the walls are held at constant temperature. The problem will be introduced into cases; the first one assuming uniform inlet temperature at $X = 0$ presenting the results downstream the flow, the second, assuming the temperature to be constant at $x = -\infty$. The results will show the effect of the upstream on the inlet temperature at $X = 0$, also the results for downstream the flow $0 < X < \infty$ will be shown. The stability analysis for the proposed method is detailed in^[20].

1. Analysis and governing equations

The heat transfer is presented as follow:

$$\frac{\partial T}{\partial t} + u \frac{\partial T}{\partial x} = \alpha \left(\frac{\partial^2 T}{\partial x^2} + \frac{\partial^2 T}{\partial y^2} \right) \quad (1)$$

Where α is the “thermal diffusivity”, u is the velocity component, the schematic of the flow is shown in Fig.

1.The boundary conditions are;

$$T(0, y, \tau) = T_o, \quad T(\infty, y, 0) = T_w, \quad \frac{\partial T}{\partial y}(x, 0, \tau) = 0, \quad T(x, \pm y_o, 0) = T_w, \quad T(x, y, 0) = T_o \quad (2)$$

Where T_o and T_w are “the upstream temperature and the wall temperature”, respectively.

The non-dimensional parameters are;

$$\theta = \frac{T - T_o}{T_w - T_o}, \quad De = 4 * y_o, \quad X = \frac{x}{De}, \quad Y = \frac{y}{De}, \quad U = \frac{u}{U_o}, \quad \tau = \frac{U_o}{De} * t \quad (3)$$

Where U_o and De are the characteristic velocity and the effective diameter. τ is non-dimensional time X, Y are non-

dimensional locations. the heat transfer equation in non-dimensional form is

$$\frac{\partial \theta}{\partial \tau} + U \frac{\partial \theta}{\partial X} = \frac{1}{Pe} \left(\frac{\partial^2 \theta}{\partial X^2} + \frac{\partial^2 \theta}{\partial Y^2} \right) \quad (4)$$

The fully developed flow considering ,so the parabolic form of the velocity is:

$$U = 1.5(1 - (y/y_0)^2) \quad (5)$$

The local value of bulk temperature is:

$$\theta_{mx} = \frac{\int_0^{y_o/De} \theta U dY}{\int_0^{y_o/De} U dY} \quad (6)$$

The local Nusselt number Nu_x is

$$Nu_x = \frac{h_x De}{\lambda} = \frac{-1}{1 - \theta_{mx}} \frac{\partial \theta}{\partial Y} \Big|_{Y=0.25} \quad (7)$$

The average value bulk temperature is:

$$\bar{\theta}_{mx} = \frac{1}{X} \int_0^X \theta_{mx} dX \quad (8)$$

The average value of the Nusselt number, \overline{Nu}_x , is

$$\overline{Nu}_x = \frac{\bar{h}_x De}{\lambda} = \frac{-1}{X(1 - \bar{\theta}_{mx})} \int_0^X \frac{\partial \theta}{\partial Y} \Big|_{Y=0.25} dX \quad (9)$$

2. The proposed Scheme

The first order of time derivative $\delta f / \delta t$ and the second-order derivatives $\delta^2 f / \delta x^2$, $\delta^2 f / \delta y^2$ and $\delta^2 f / \delta z^2$ are done using two-time level derivative as follow:

$$\frac{\partial f_{i,j,k}^n}{\partial t} = \frac{f_{i,j,k}^{n+1} - f_{i,j,k}^n}{\Delta t} + O(\Delta t) \quad (10)$$

$$\frac{\partial^2 f_{i,j,k}^n}{\partial x^2} = \frac{(f_{i+1,j,k}^n - f_{i,j,k}^n) - (f_{i,j,k}^{n+1} - f_{i-1,j,k}^{n+1})}{\Delta x^2} + O\left(\frac{\Delta t}{\Delta x}, \Delta x^2\right) \quad (11)$$

$$\frac{\partial^2 f_{i,j,k}^n}{\partial y^2} = \frac{(f_{i,j+1,k}^n - f_{i,j,k}^n) - (f_{i,j,k}^{n+1} - f_{i,j-1,k}^{n+1})}{\Delta y^2} + O\left(\frac{\Delta t}{\Delta y}, \Delta y^2\right) \quad (12)$$

$$\frac{\partial^2 f_{i,j,k}^n}{\partial z^2} = \frac{(f_{i,j,k+1}^n - f_{i,j,k}^n) - (f_{i,j,k}^{n+1} - f_{i,j,k-1}^{n+1})}{\Delta z^2} + O\left(\frac{\Delta t}{\Delta z}, \Delta z^2\right) \quad (13)$$

Also $\delta f / \delta x$, $\delta f / \delta y$ and $\delta f / \delta z$ using the two-time-level backward or forward differences as follow;

$$\frac{\partial f_{i,j,k}^n}{\partial z} = \frac{f_{i,j+1,k}^n - f_{i,j,k}^{n+1}}{\Delta z} \quad w \leq 0 \quad (19)$$

$$\frac{\partial f_{i,j,k}^n}{\partial x} = \frac{f_{i,j,k}^n - f_{i-1,j,k}^{n+1}}{\Delta x} \quad u \geq 0 \quad (14)$$

$$\frac{\partial f_{i,j,k}^n}{\partial y} = \frac{f_{i,j,k}^n - f_{i,j-1,k}^{n+1}}{\Delta y} \quad v \geq 0 \quad (15)$$

$$\frac{\partial f_{i,j,k}^n}{\partial z} = \frac{f_{i,j,k}^n - f_{i,j,k-1}^{n+1}}{\Delta z} \quad w \geq 0 \quad (16)$$

(or)

$$\frac{\partial f_{i,j,k}^n}{\partial x} = \frac{f_{i+1,j,k}^n - f_{i,j,k}^{n+1}}{\Delta x} \quad u \leq 0 \quad (17)$$

$$\frac{\partial f_{i,j,k}^n}{\partial y} = \frac{f_{i,j+1,k}^n - f_{i,j,k}^{n+1}}{\Delta y} \quad v \leq 0 \quad (18)$$

The scheme is stable under any condition^[20]. No restrictions for spatial increments $\Delta x'$ or the time $\Delta t'$. (i, j) is used instead of (x, y) to be subscript for variable, $(i + 1)$ instead of $(x + \Delta x)$ and instead of $(i - 1)$, and $(x - \Delta x)$ and by the same way (n) represents the time level (t) as shown in figure 3.

3. The downstream results

Figure 4 displays the local bulk temperature, θ_{mx} , versus x/De for $Pe = 1000, 5000, 10000, 100000, 300000$ and 700000 to show the effect of the Peclet number on the local bulk temperature. As shown in the figure the rate of heat transfer at low Peclet number is very high and decreases as the Peclet number increases. Figure 5 displays the same results of local bulk temperature. All the graphs coincided at figure 4 when the local bulk temperature versus $X^* = (x / De) / Pe$.

Figure 6 displays the local Nusselt number versus (x/De) for $Pe = 1000, 5000, 10000, 100000, 300000$ and 700000 , respectively. The Peclet number effect is shown.

For one value of (x/De) , Nux increases with increasing Pe value. In the region of fully developed, the Nux tends to 7.5407, in agree with Graetz problem where the effect of disappear.

The same results which shown in figure 6 are displayed again in the figure 7 but versus $(x/De) / Pe$, to show that the curves do not coincide such as the case of neglecting the axial conduction.

Figure 8 displays the averaged bulk temperature versus x/De for $Pe = 1000, 5000, 10000, 100000, 300000$ and 700000 , respectively. For each value of x/De , the $\bar{\theta}_{mx}$ value becomes smaller as greater Pe value is, the smaller is. While at figure 9 all the curves coincided versus $(x/De) / Pe$.

Figure 10 displays the results of the average Nusselt number versus x/De for $Pe = 1000, 5000, 10000, 100000, 300000$, and 700000 , respectively. The effect of the Peclet number Pe , on the average value of Nusselt number is presented. For each value of x/De , the \bar{Nux} value increases with increasing Pe . In the region of fully developed, the value of \bar{Nux} approaches to 7.5407, in agree with Graetz problem where the effect of Pe disappear.

Figure 11 displays the average Nusselt number versus

x/De for Pe for $Pe = 1000, 5000, 10000, 100000, 300000$, and 700000 , respectively. The curves do not coincide such as in classical Graetz problem, to demonstrate the effect of the axial heat conduction on the heat transfer from the wall at the entrance.

The increase in Peclet number decreases the effect of the axial heat diffusion as shown in figures 12 and 13. Figure 12 displays axial heat conduction effect for three groups of Nusselt number versus x/De for $Pe = 500, 1000$ and 5000 . Including the axial heat conduction increases the local Nusselt number.

Figure 13 also show at high Peclet numbers the effect of axial heat conduction in three groups of Nusselt number versus x/De for $Pe = 500, 1000, 5000$ and 10000 , Including the axial heat conduction increases the local Nusselt number.

Figures 12 and 13 demonstrate that, first; the axial heat conduction increases the heat transfer to the wall increases at the entrance, second; with the increase of the Peclet number, the effect of axial heat conduction decreases. And finally, when Peclet number is larger than 1000, this effect of the axial diffusion term almost vanishes.

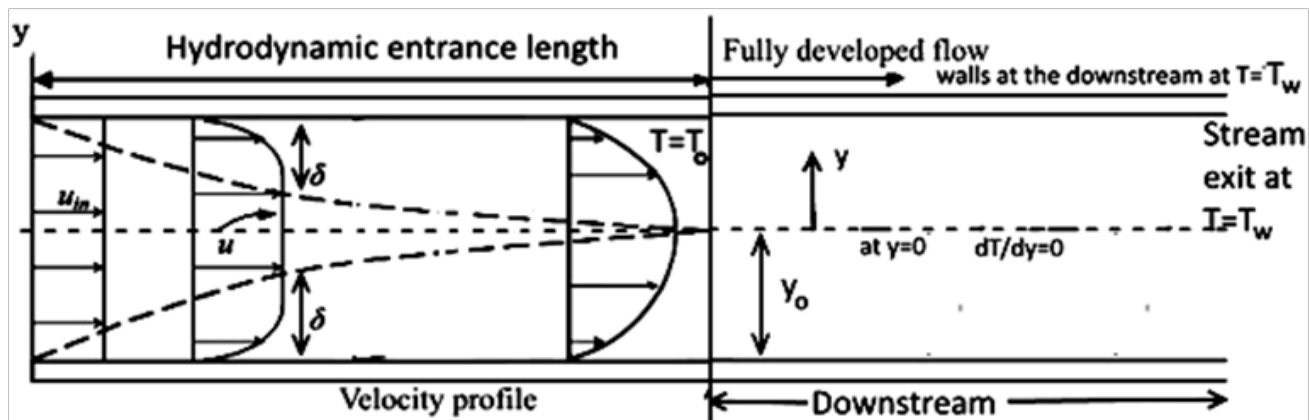


Fig. 1: The Graetz problem description

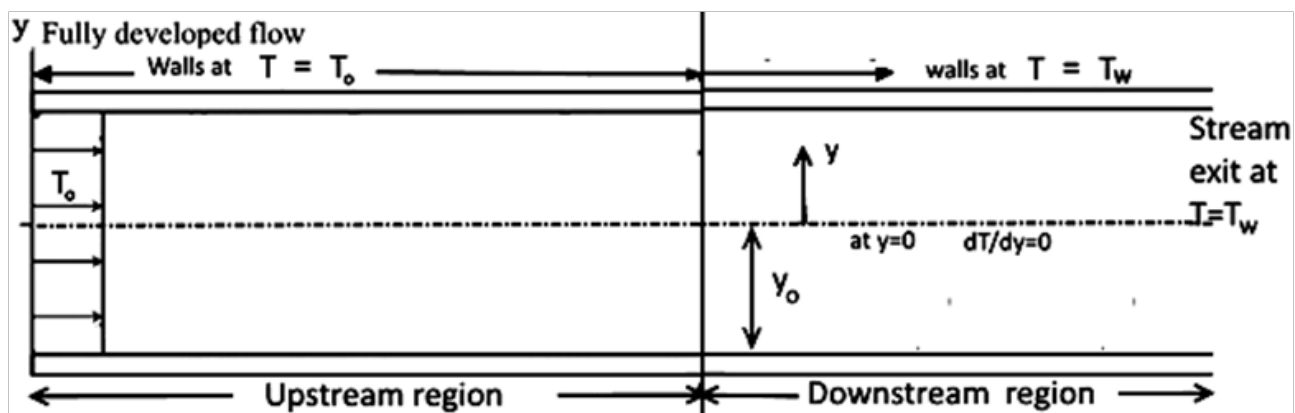


Fig. 2: Upstream diffusion outline

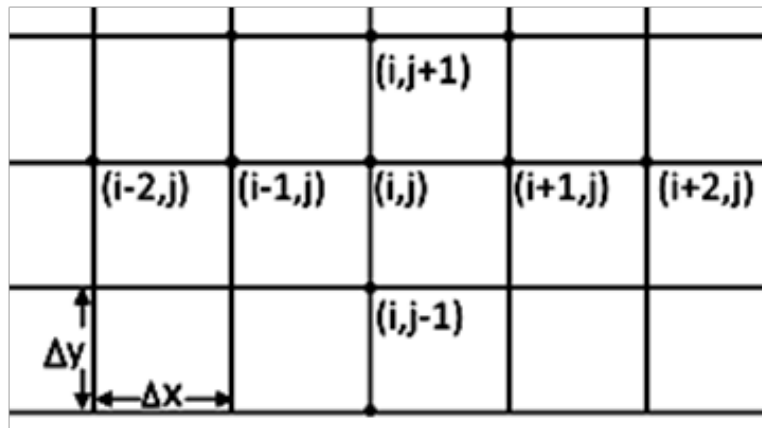


Fig. 3: Notations for the discretization mesh

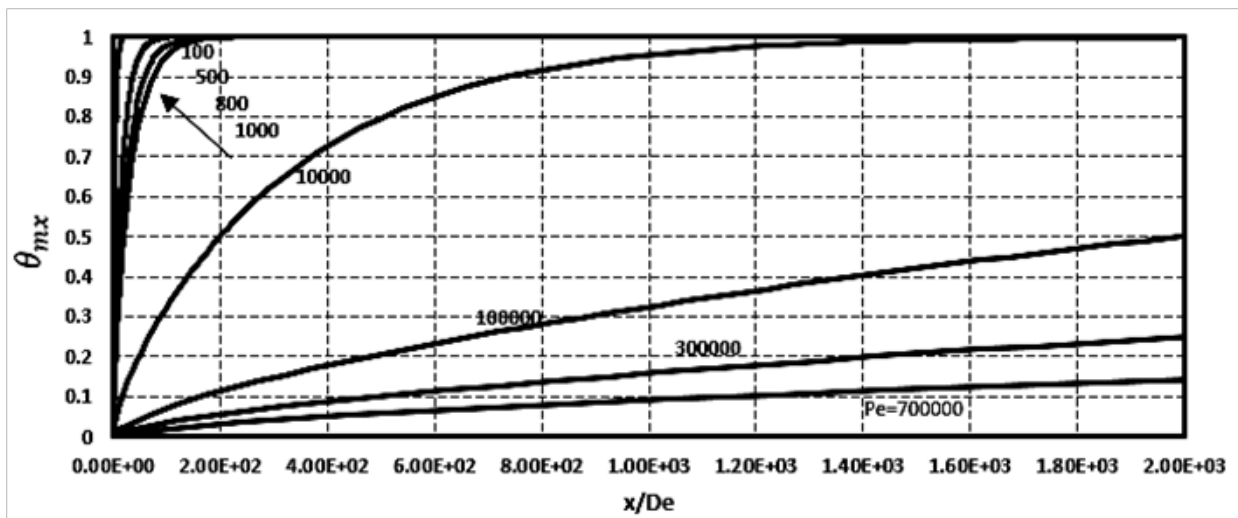


Fig. 4: The local bulk temperature θ_{mx} versus x/De for T-problem with axial diffusion term

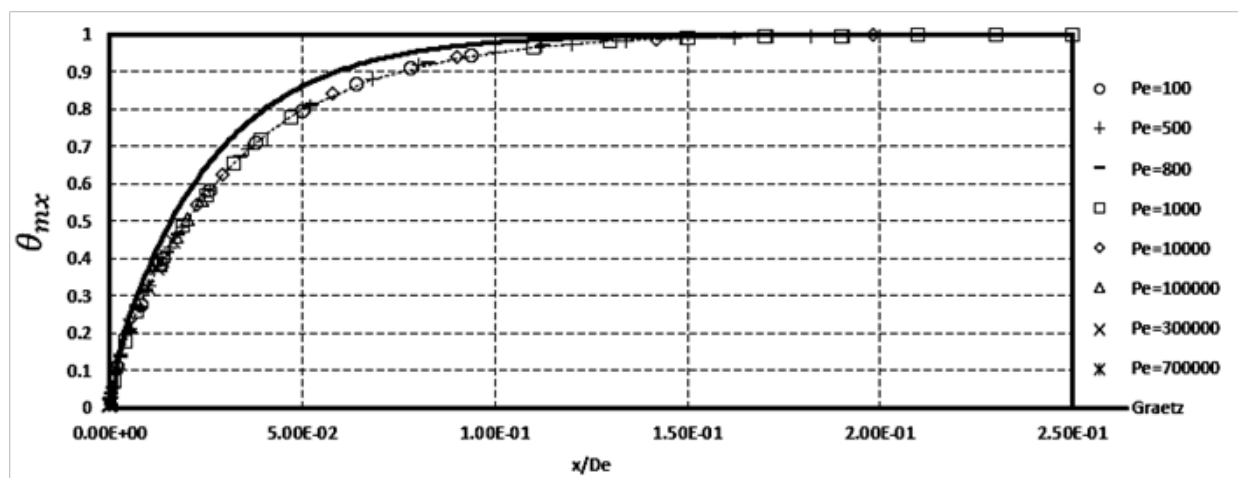


Fig. 5: The local bulk temperature θ_{mx} versus $(x/De)/Pe$ for T-problem with axial diffusion term

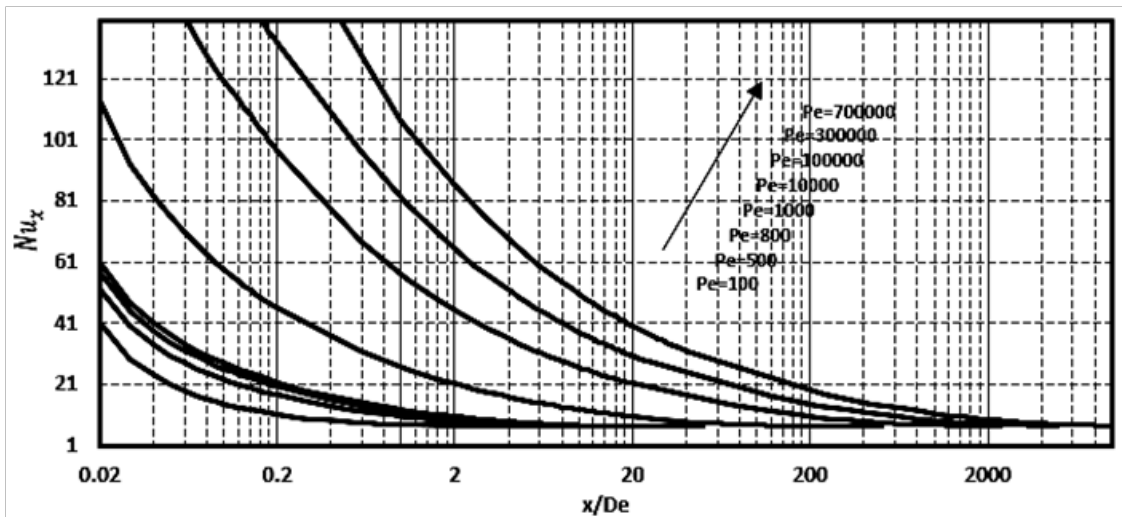


Fig. 6: The local value of Nusselt number Nu_x versus x/De for T-problem with axial diffusion term

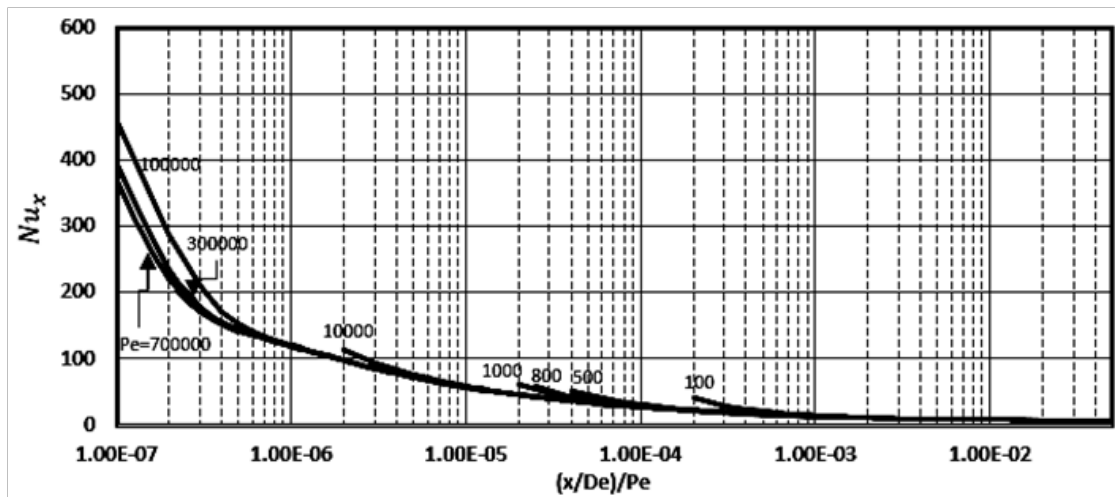


Fig. 7: The local value of Nusselt number Nu_x versus $(x/De)/Pe$ for T-problem with axial diffusion term

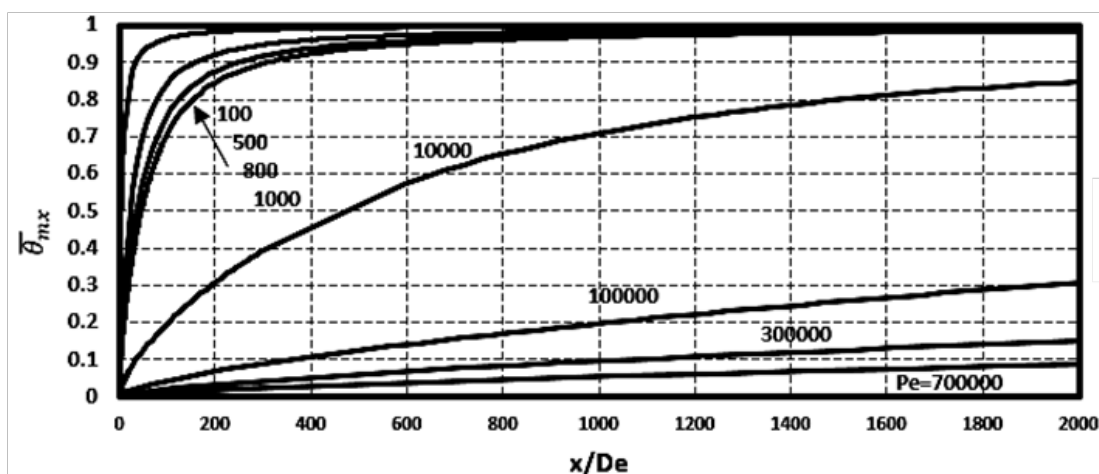


Fig. 8: The averaged bulk temperature θ_{mx}^- versus x/De for T-problem with axial diffusion term

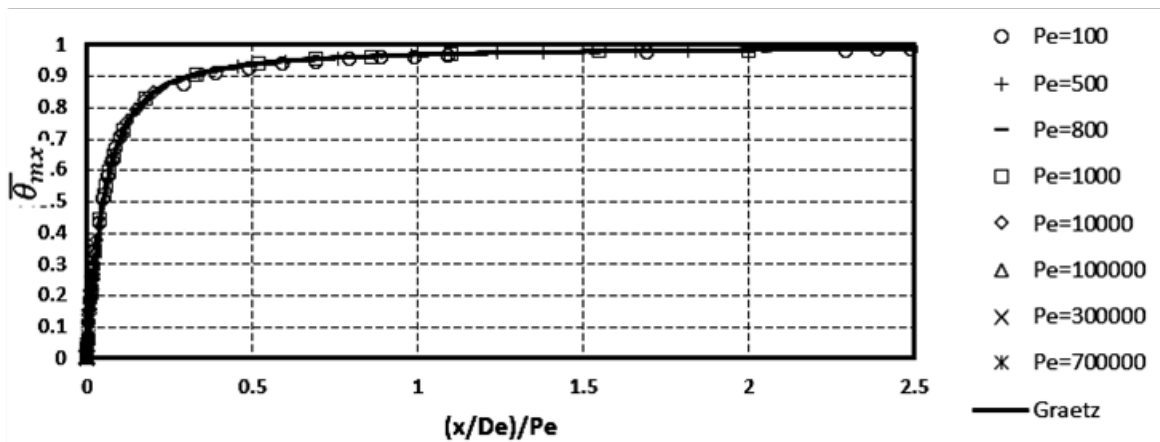


Fig. 9: The averaged bulk temperature $\bar{\theta}_{mx}$ versus $(x/De)/Pe$ for T-problem with axial diffusion

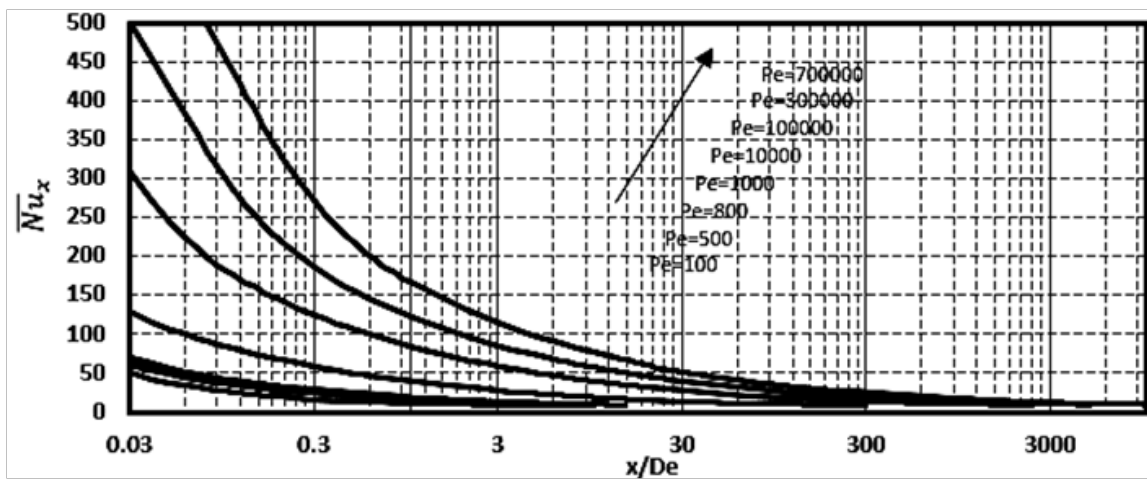


Fig. 10: The averaged value of Nusselt number \bar{Nu}_x versus x/De for T-problem with axial diffusion term

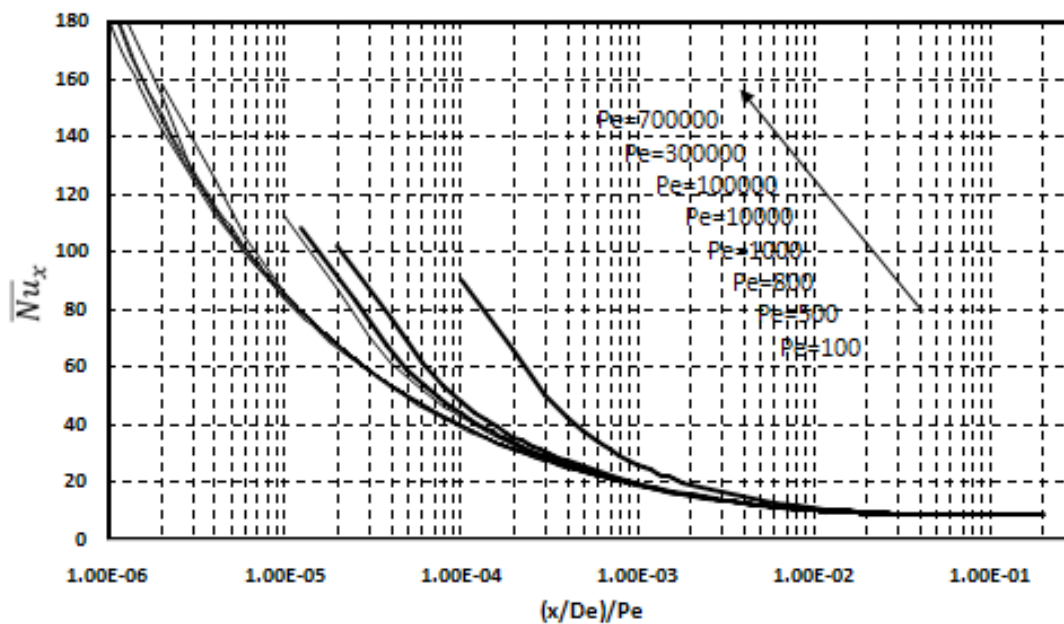


Fig. 11: The averaged Nusselt number \bar{Nu}_x versus $(x/De)/Pe$ for T-problem with axial diffusion

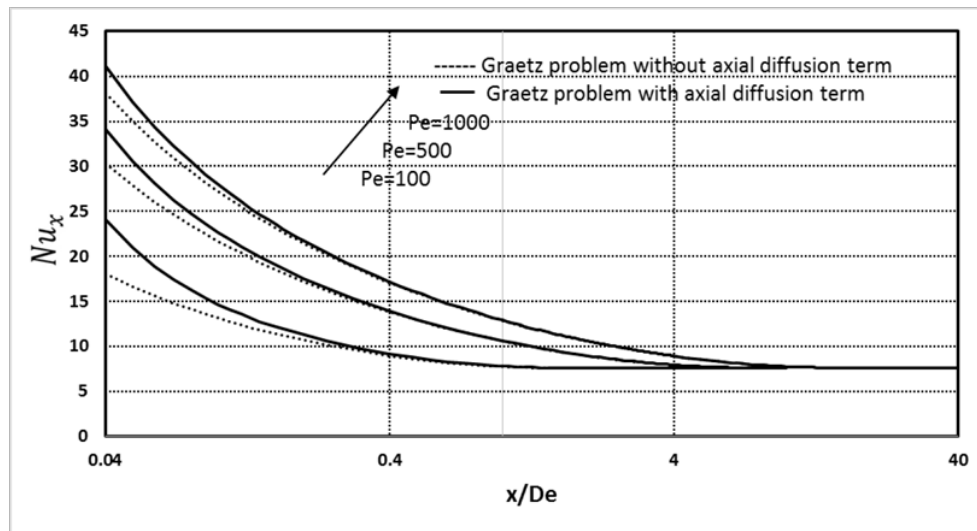


Fig. 12: Effect of axial heat conduction for T-problem with axial diffusion term at low Pe numbers.

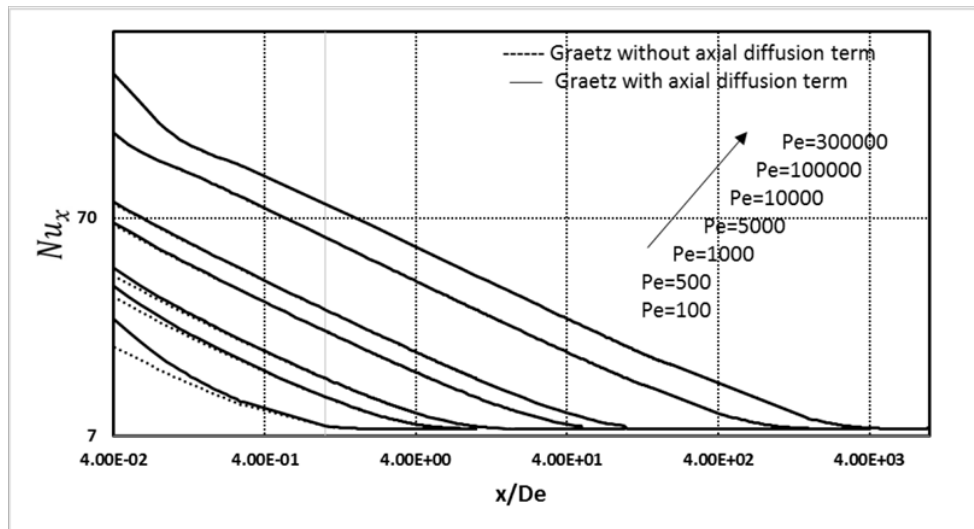


Fig. 13: Effect of axial heat conduction for T-problem with axial diffusion term at high Pe numbers (log-log scale)

4. Thermal entry length

A fully developed heat flow between two infinite parallel plates can be considered in the following situation. If the plates are held at constant wall temperature, such as in the journal bearings, then the bulk temperature of the fluid increases steadily at a fixed rate along the flow direction. The fully developed heat flow at a distance away from the fluid entrance is achieved, when the fluid heat transfer coefficient, h , be constant $h = (\lambda / De) * Nu_x$, as well as the temperature profile along the flow is the same shape. The definition of this distance is called the thermal entry length or thermal entrance length. This distance is important in designing an efficient heat transfer system. For T-problem, the thermal entrance length is estimated based on the fully developed value of the local Nusselt number. In this case the thermal entrance length is calculated at the distance

from the entry to the point at which the following relation is accomplished.

$$\frac{Nu_x}{7.5407} = 1.01 \quad (21)$$

Where 7.5407 is the local Nusselt number for the T-problem (flow between parallel plates) when the heat flow is fully developed. Figure 12 displays the thermal entry length versus the Pe value, The thermal entry length can be calculated analytical using the following proposed empirical correlation:

$$X_{th} = 1.704 * Exp(Pe^{-1.639}) - 1.69 \quad (22)$$

Equation 21 gives a good agreement with the results obtained numerically for the T-problem with axial diffusion term, the maximum error for this equation is 0.5%.

5. The stability analysis for the proposed scheme

The Fourier expansion is:

$$f_i^n = \zeta^n e^{i\gamma x} = \zeta^n (\cos \gamma x + i \sin \gamma x) \quad (22)$$

$$f_i^{n+1} \left(1 + \frac{c\Delta t}{\Delta x^2}\right) - f_{i-1}^{n+1} \left(\frac{U\Delta t}{\Delta x} + \frac{c\Delta t}{\Delta x^2}\right) = f_i^n \left(1 - \frac{U\Delta t}{\Delta x} - \frac{c\Delta t}{\Delta x^2}\right) + f_{i+1}^n \left(\frac{c\Delta t}{\Delta x^2}\right) \quad (23)$$

Then ζ^{n+1} and ζ^n in equation (23);

$$\zeta^{n+1} \left(1 + \frac{c\Delta t}{\Delta x^2}\right) - \zeta^{n+1} \left(\frac{U\Delta t}{\Delta x} + \frac{c\Delta t}{\Delta x^2}\right) e^{-i\gamma\Delta x} = \zeta^n \left(1 - \frac{U\Delta t}{\Delta x} - \frac{c\Delta t}{\Delta x^2}\right) + \zeta^n \left(\frac{c\Delta t}{\Delta x^2}\right) e^{i\gamma\Delta x} \quad (24)$$

The numerical solution will be bounded as μ^n and μ^{n+1} , according to the test of Von-Neumann, if the amplification factor μ^n is bounded, which need

$$\max|\mu^n| \leq 1$$

Where u^n is

$$\mu^n = \frac{\zeta^{n+1}}{\zeta^n} = \frac{\left(1 - \frac{U\Delta t}{\Delta x} - \frac{c\Delta t}{\Delta x^2}\right) + \left(\frac{c\Delta t}{\Delta x^2}\right) e^{i\gamma\Delta x}}{\left(1 + \frac{c\Delta t}{\Delta x^2}\right) - \left(\frac{U\Delta t}{\Delta x} + \frac{c\Delta t}{\Delta x^2}\right) e^{-i\gamma\Delta x}} \quad (25)$$

Considering the following parameters to simplify equation (25);

$$v = \frac{U\Delta t}{\Delta x} \quad \text{and} \quad r = \frac{c\Delta t}{\Delta x^2} \quad (26)$$

Then the u^n is given by;

$$\mu^n = \frac{(1 - v - r) + (r) e^{i\gamma\Delta x}}{(1 + r) - (v + r) e^{-i\gamma\Delta x}} \quad (27)$$

The absolute magnitude of u^n is

$$|\mu^n|^2 = \frac{(1 - r - v)^2 + r^2 + 2(1 - r - v)r \cos \gamma\Delta x}{(1 + r)^2 + (r + v)^2 - 2(1 + r)(r + v) \cos \gamma\Delta x} = \frac{A}{B} \quad (28)$$

To get the maximum value of u^n , differentiate the right-hand side of equation (28) with respect to $(\gamma\Delta x)$ as following.

$$\frac{\partial |\mu^n|^2}{\partial \gamma\Delta x} = \frac{\left(\frac{\partial A}{\partial \gamma\Delta x}\right) B - \left(\frac{\partial B}{\partial \gamma\Delta x}\right) A}{B^2} = 0 \quad (29)$$

Where:

$$\begin{aligned} \frac{\partial B}{\partial \gamma\Delta x} &= 2(1 + r)(r + v) \sin \gamma\Delta x \\ \frac{\partial A}{\partial \gamma\Delta x} &= -2r(1 - r - v) \sin \gamma\Delta x \end{aligned} \quad (30)$$

Substitution at equation (29) the final result is:

$$[(2r + v)(1 - v)^2] \sin \gamma\Delta x = 0 \quad (31)$$

Equation (31) shows that u^n is minimum or maximum if;

$$\begin{aligned} 1- \sin \gamma\Delta x = 0 &\rightarrow \cos \gamma\Delta x = \pm 1 \\ 1.1- \cos \gamma\Delta x = 1 &\text{ then } |\mu^n|^2 = 1 \\ 1.2- \cos \gamma\Delta x = -1 & \end{aligned} \quad (32)$$

$$|\mu^n|^2 = \frac{1 - 4r - 2v + 4r^2 + 4rv + v^2}{1 + 4r + 2v + 4r^2 + 4rv + v^2}$$

The first condition makes $|u^n| \leq 1$, but the second condition makes $|u^n| \leq 1$ if $v > 0$ but if $v < 0$ provided that $\Delta x < 2/(Re * U_{max})$.

$$2- v = 1 \quad (33)$$

$$|\mu^n|^2 = \frac{r^2}{(1 + r)^2}$$

Then the scheme is stable.

$$\begin{aligned} 3- 2r + v = 1 &\rightarrow v = -2r \\ |\mu^n|^2 &= \frac{(1 - r + 2r)^2 + r^2 + 2(1 - r + 2r)r \cos \gamma\Delta x}{(1 + r)^2 + (r - 2r)^2 - 2(1 + r)(r + 2r) \cos \gamma\Delta x} \end{aligned} \quad (34)$$



According to the result tabulated in table 1, for Barakat RW convection term, the backward representation is suitable for the positive u-velocity only as represented from the above conditions, while for the negative u-velocity $\Delta x < 2 / Re * U_{max}$ should be satisfied. Also,

in the same way for negative velocity, when using Barakat RW the convection term by the forward representation it is unconditionally stable for negative u-velocity, while for positive u-velocity $\Delta x < 2 / Re * U_{max}$ should be satisfied.

Table 1: T-problem with axial diffusion term for positive and negative velocity

$(x/De) Pe$	θ_m with (+u)	θ_m with (-u)	θ_m^- with (+u)	θ_m with (-u)
0	0	0	0	0
0.0005	0.044579	0.044579	0.025864	0.025864
0.003	0.147941	0.147941	0.088739	0.088739
0.006	0.232969	0.232969	0.140469	0.140469
0.008	0.280885	0.280885	0.169689	0.169689
0.01	0.324474	0.324474	0.196349	0.196349
0.012	0.364751	0.364751	0.2211	0.2211
0.013	0.383835	0.383835	0.232889	0.232889
0.014	0.402285	0.402285	0.244333	0.244333
0.015	0.420139	0.420139	0.255462	0.255462
0.016	0.437428	0.437428	0.266297	0.266297
0.017	0.454179	0.454179	0.276859	0.276859
0.018	0.470415	0.470415	0.287163	0.287163
0.019	0.486158	0.486158	0.297224	0.297224
0.02	0.501424	0.501424	0.307055	0.307055

6. CONCLUSION

The proposed numerical method extends Barakat-Clark (ADE) method to solve the transport equation which represents the rightward method. The unsteady term presented using two-time level derivative at n and n+1 combined with backward derivative i and i-1. As a sample of the transport equation, the heat equation is considered in unsteady form. The heat equation contains the unsteady term and the axial heat term. The heat transfers within flow between two parallel plates. The equation is transformed into dimensionless form, the results for different dimensionless numbers are presented, and the results show the following:

- The local bulk temperature shows rapid change at low Peclet numbers (<1000) and as the Peclet number increases the change of the temperature became slow.

- The proposed numerical method presented rapid and stable solutions at high Peclet numbers (up to $Pe=70000$)

- The proposed method presented a stable and rapid solution for the local Nusselt number and shows Nusselt number variation at different values of Peclet numbers.

- The solution for averaged values of bulk temperature and the averaged values of Nusselt number shows good agreement with the Graetz problem.

- The results demonstrated that, in the fully developed region, the values of Pe has no effect on Nusselt number.

- The second order term $\partial^2 T / \partial x^2$ is of an important order magnitude in the entrance, or the developing region only. It is of unimportant order of magnitude in the region of fully developed flow.

- The thermal entrance length is presented graphically, and an empirical correlation is induced.

- The stability analysis shows that the proposed scheme is unconditionally stable.

7. REFERENCES

- [1] H.C. Agrawal, Heat transfer in laminar flow between parallel plates at small Peclet numbers, *appl. Sci. Res.*, Vol.9, pp. 177-189, 1960
- [2] F.W. Schmidt and B. Zeldin, Laminar heat transfer in the entrance region of Ducts, *Appl. Sci. Res.*, Vol. 23, pp. 73-94, 1970
- [3] R.K. Shah, Al. L. London, Laminar flow forced convection in ducts, Supplement 1 to advances in Heat transfer, Academic Press, New York, 1978.
- [4] Y. Taitel and A. Tamir, Application of the integral method to flows with axial diffusion, Vol. 15, pp. 733-740, 1972
- [5] Y. Taitel and A. Tamir, effects of Upstream and downstream boundary conditions on heat mass transfer with axial diffusion, vol. 16, pp. 359-369, 1973.
- [6] D. Hennecke, Heat transfer by Hagen-poiseuille flow in the thermal development region with axial conduction, *Warme and Stoffubertragung*, Vol. 1, pp. 177-184, 1968
- [7] B.Vick, M.N.Özişik, and D.F.Ullrich, Effects of axial conduction in laminar tube flow with convective boundaries, *J. of Franklin institute*, Vol. 316, pp. 159-173, 1983
- [8] T.V. Nguyen, Laminar heat transfer for thermally developing flow in ducts, *Int. J. of Heat and Mass Transfer*, Vol. 35, pp. 1733-1741, 1992
- [9] D.A. Nield and A.V. Kuznetsov, Ming Xiong, Thermally developing forced convection in a porous medium: parallel plate channel with walls

at uniform temperature, with axial conduction and viscous dissipation effects, Int. J. of Heat and Mass Transfer, Vol. 46, pp. 643-651, 2003.

[10] D. Nield, Forced convection in a parallel plate channel with asymmetric heating, Int. J. of heat and mass transfer, Vol. 47, pp. 5609-5612, 2004.

[12] MI. Hasan and HM. Hasan, Study of the axial heat conduction in parallel flow microchannel heat exchanger, J. of King Saud university-Engineering science, Vol. 26, pp. 122-131, 2014.

[13] H.Ling and X.Shao, Effects of axial heat conduction and viscous dissipation on heat transfer in circular micro-channels, Int. J. of thermal science, Vol. 66, pp. 34-41, 2013.

[14] B. Weigand and M. Abdelmoula, Axial heat conduction effects in the entrance region of laminar duct flows: Correlations for local Nusselt number, Int. Comm. In Heat and Mass Transfer, Vol. 51, pp. 45-50, 2014.

[15] H. Yang, J. Wen, X. Gu, Y. Liu, S. Wang, W. Cai, Y. Li, A mathematical model for flow maldistribution study in a parallel plate-fin heat exchanger, Applied Thermal Engineering, Vol. 121, pp. 462-472, 2017.

[16] Víctor J. Llorente , A. Pascau, Numerical simulations of

magnetorheological fluids flowing between two fixed parallel plates, Applied Mathematical Modelling, Vol. 74, pp. 151-169, 2019.

[17] Z. Wu, P. Mirbod, Instability analysis of the flow between two parallel plates where the bottom one coated with porous media, Advances in Water Resources, Vol. 130, pp. 221-228, 2019.

[18] S. K. Kim, Forced convection heat transfer for the fully-developed laminar flow of the cross fluid between parallel plates, Journal of Non-Newtonian Fluid Mechanics, Vol. 276, 104226, 2020.

[19] F. Mentzoni, T. Kristiansen, Two-dimensional experimental and numerical investigations of parallel perforated plates in oscillating and orbital flows, Applied Ocean Research Vol. 97, 102042, 2020.

[20] Barakat, H.Z. and Clark J.A., On the solution of the diffusion equations by numerical methods, J. Heat transfer, Vol. 88, pp. 421-427, 1966.

[21] Saad, Hany, and Hamada G. Asker. "An unconditionally stable finite-difference method for the solution of multi-dimensional transport equation." Ain Shams Engineering Journal vol.12, no. 1 (2021): 807-820.

Nomenclature	
c	Arbitrary coefficient [-]
C_p	Specific heat at constant pressure [J/kg.K]
dx, dy	Spatial mesh size [m]
De	Effective diameter [m]
f	Dependent variable [-]
L	Characteristic length [m]
n	Constant [-]
Nux	Local Nusselt number [-]
\overline{Nux}	Averaged Nusselt number [-]
Pe	Peclet number [-]
Pr	Prandtl number [-]
Re	Reynold's number [-]
T	Temperature [K]
T_o	Entering stream temperature [K]
T_w	Wall temperature [K]
t	Time [s]
u, v, w	Velocity components [m/s]
U	Dimensionless x- component of velocity [m/s]
U_o	characteristic velocity; upstream velocity [m/s]
y_o	Gap height [m]
x, y, z	Spatial location [m]
Δ	Difference
α	Thermal diffusivity [m ² /s]
θ	Dimensionless temperature [-]
θ_{mx}	Local Bulk temperature [-]
$\bar{\theta}_{mx}$	Averaged bulk temperature [-]
μ	Kinematic viscosity [m ² /s]
τ	Dimensionless time [-]
Superscripts	
n	trial number
subscripts	
i, j, k	counters